



Optimal Control Structure Selection Based on Economics for Continuous Cross-Flow Grain Dryer

Agustín Bottari^{a,b} and Lautaro Braccia^{b,c}

^aInstituto de Investigaciones en Ingeniería Ambiental, Química y Biotecnología Aplicada (INGEBIO), Facultad de Química e Ingeniería del Rosario, Pontificia Universidad Católica Argentina (UCA), Rosario, Argentina; ^bConsejo Nacional de Investigaciones Científicas y Técnicas (CONICET), Buenos Aires, Argentina; ^cGrupo de Ingeniería de Sistemas de Procesos (GISP), Centro Franco-Argentino de Ciencias de la Información y de Sistemas (CIFASIS), Rosario, Argentina

ABSTRACT

In this work, we present the control structure selection problem based on steady-state economics applied to a continuous cross-flow grain dryer model. The optimal selection of the controlled and manipulated variables and their set-points can be obtained for various external disturbance scenarios if an appropriate mathematical programming problem is formulated. Simulation results show that the economics performance of classical open loop and closed loop structure used for dryer control can be improved by the use of linear combination of controlled variables and also by the use of a hierarchical control structure. In addition, we study several alternatives (sub-optimal) control structures that show an acceptable economic performance.

ARTICLE HISTORY

Received 27 October 2022
Revised 28 December 2022
Accepted 9 January 2023

KEYWORDS

Dryer; control; optimization

1. Introduction




The objective of the drying process in any industrial plant is to produce a solid product at minimum operation cost while ensuring that different technical, chemical, and biological parameters are within specific quality limits. The drying process is a highly energy consuming unit operation in grain processing plants and food industries that can represent around 10–15% of all industrial energy requirements [1]. Finding the (possibly changing) operating point that satisfies the quantity and quality production requirements while the operation costs or energy consumption is minimized is one of the most interesting tasks in process operation. In this sense, the use of automatic control strategies generally allows the industrial processes to achieve the production objectives while the operating costs are reduced.

The drying process involves a large number of inputs variables (e.g., heating rate, solids feed rate, air-flow rate, and rotational speed), output variables (e.g., dried-product moisture content, exhaust air temperature, temperature of the air-product mixture, exhaust air humidity, and product quality as color, flavor, textures, etc.), and disturbances that affect performance

of the dryers (e.g., ambient air temperature, ambient air humidity, feed moisture content, and feed composition). Also, it is important to note that there is a high level of interaction between the drying process variables. The highly interactive multiple input-output (MIMO) system in combination with a typically non-linear dynamics and the presence of time delay and time-varying parameters make the drying process operation and control a difficult task.

A large number of control strategies designed for different types of dryers and products can be found in the literature [2]. The works include: i) feedback control [3] and feedforward-feedback control [4–6], and ii) advanced control techniques such as model-based control [7, 8], neural net controllers [9] and fuzzy logic controllers [10, 11]. For the main technological advances in dryers the reader is referred to the works [12, 13] and for excellent reviews about drying control strategies to the works [1, 2, 14].

Generally, to design the control system in any industrial process it is first necessary to define: i) the number of levels or layers in the control system, e.g., using only regulatory control (one layer) or using regulatory control plus high-level optimization (two

CONTACT Agustín Bottari  agustinbottari@uca.edu.ar  Instituto de Investigaciones en Ingeniería Ambiental, Química y Biotecnología Aplicada (INGEBIO), Facultad de Química e Ingeniería del Rosario, Pontificia Universidad Católica Argentina (UCA), Av. Pellegrini 3314, S2002QEO, Rosario, Argentina
 Supplemental data for this article can be accessed online at <https://doi.org/10.1080/07373937.2023.2167829>.

layers), ii) the performance objectives for the layers/-system, and iii) types of control technology available. Then, the control structure is defined based on the performance objectives, technology, and layers, this is, the manipulated and controlled variables as well as the pairing and reference values are selected. It is very common that the regulatory control structure is designed based on only stability and controllability criteria, e.g., using the integral error criterion, calculating the relative gain matrix or the condition number. However, economic criteria or the existence of higher levels of control are ignored in these approaches.

The selection of the controlled variables, the manipulated variables, and the set point definition impact directly on the process operation and, therefore, on their economics and energy requirements. The control structure selection based on economic criteria is a research field that attends the following challenges: i) the optimal operation point of the plant can change in the presence of external disturbances, ii) the process constraints cannot be violated when disturbance takes place, and iii) the optimal point may change the set of active constraint for different disturbance scenarios. Two of the main economics-based strategies for control structure selection are the back-off approach [15] and the self-optimizing method [16]. Recently, in [17] the aforementioned strategies were unified in a single optimization problem. These strategies have been largely studied for a variety of chemical industrial processes like evaporation, distillation columns, chemical reactors, compressor stations, and heat exchanger networks [18]. However, to the best of our knowledge, there is no work that applied these approaches to industrial dryers.

In the drying process, the control structure is typically defined based on manufacturer recommendations, heuristic procedures, field experience, or stability/controllability criteria. Once the control structure is selected, an optimization-based approach is performed to improve the dynamic response of the process, economic performance, and/or energy consumption. Still, a sequential procedure and the use of different criteria for selection and optimization might result in a sub-optimal control system. Although the importance in a global and competitive market, a simultaneous approach for the control structure selection with controller tuning or economics operation index for industrial dryers has received little attention.

The focus of this paper is to systematically study the steady-state economic performance that the continuous grain dryer process can achieve by applying

back-off self-optimizing methods and, also, by the possible use of a hierarchical control structure with a real-time optimization layer. Based on economic criteria and a steady-state model we provide a deterministic approach to design the control structure of industrial dryers.

The rest of the work is organized as follows. In Section 2 the related theory to economic optimal operation, control structure selection approaches, and real-time optimization proposed for this work are presented. A detailed description of the selected continuous dryer model, process variables and constraints are shown in Sections 3.1 and 3.2. The proposed objective function together with the mathematical formulations of optimization problems are carried out in Sections 3.3 and 3.4. In Section 4 several alternatives control structures are designed and compared. Finally, Section 6 summarizes the conclusions, discussions, and future work.

2. Theory

2.1. Optimal operation point problem

The open loop behavior of an industrial plant can be represented by a system of differential and algebraic equations:

$$\mathbf{f}_D(\mathbf{x}, \mathbf{x}, \mathbf{w}, \mathbf{u}, \mathbf{d}) = 0, \quad (1a)$$

$$\mathbf{f}_A(\mathbf{x}, \mathbf{w}, \mathbf{u}, \mathbf{d}) = 0, \quad (1b)$$

$$\mathbf{y} = \mathbf{F}(\mathbf{x}, \mathbf{w}, \mathbf{u}, \mathbf{d}), \quad (1c)$$

where \mathbf{f}_D is the vector of dimension n_x that contains the differential equations of the model, \mathbf{f}_A is the vector of dimension n_w that contains the algebraic equations of the model, and $\mathbf{y} \in \mathbb{R}^{n_y}$ is the vector of output variables (measurable variables). The vector of state variables is $\mathbf{x} \in \mathbb{R}^{n_x}$, the vector with algebraic variables is $\mathbf{w} \in \mathbb{R}^{n_w}$, the input or decision variable is $\mathbf{u} \in \mathbb{R}^{n_u}$, and $\mathbf{d} \in \mathbb{R}^{n_d}$ is the vector of disturbances variables.

Generally, continuous plants are designed for a steady-state operation, i.e., setting $\dot{\mathbf{x}} = 0$ in Eq. (1a). The optimal steady-state operation point can be obtained by solving a nonlinear programming problem (NLP):

$$\min_{\mathbf{x}, \mathbf{w}, \mathbf{u}} \Phi(\mathbf{x}, \mathbf{w}, \mathbf{u}, \mathbf{d}) \quad (2a)$$

$$\text{s.t. } \mathbf{f}_D(0, \mathbf{x}, \mathbf{w}, \mathbf{u}, \mathbf{d}) = 0, \quad (2b)$$

$$\mathbf{f}_A(\mathbf{x}, \mathbf{w}, \mathbf{u}, \mathbf{d}) = 0, \quad (2c)$$

$$\mathbf{y}^L \leq \mathbf{y} = \mathbf{F}(\mathbf{x}, \mathbf{w}, \mathbf{u}, \mathbf{d}) \leq \mathbf{y}^U, \quad (2d)$$

$$\mathbf{u}^L \leq \mathbf{u} \leq \mathbf{u}^U, \quad (2e)$$

where Φ is the objective function (the economic operation cost of the drying process for this work). While the parameters \mathbf{y}^L and \mathbf{y}^U are the lower and upper bounds, respectively, for output variables (Eq. (2d)), \mathbf{u}^L and \mathbf{u}^U are the lower and upper bounds for input variables (Eq. (2e)).

For given values of \mathbf{u} and \mathbf{d} , it is assumed that the solution of the system (2b, 2c) can be expressed via a steady-state mapping:

$$(\mathbf{x}, \mathbf{w}) = \zeta(\mathbf{u}, \mathbf{d}) \quad (3)$$

where ζ is the steady-state mapping operator between (\mathbf{u}, \mathbf{d}) and (\mathbf{x}, \mathbf{w}) .

Similarly, the steady-state input-output mapping between $\mathbf{y}(\mathbf{u}, \mathbf{d})$ and $\Phi(\mathbf{u}, \mathbf{d})$ can be defined as following:

$$\Phi(\mathbf{u}, \mathbf{d}) = \Phi(\zeta(\mathbf{u}, \mathbf{d}), \mathbf{u}, \mathbf{d}), \quad (4a)$$

$$\mathbf{y}(\mathbf{u}, \mathbf{d}) = \mathbf{F}(\zeta(\mathbf{u}, \mathbf{d}), \mathbf{u}, \mathbf{d}). \quad (4b)$$

Using these mappings, the problem (2) can be written compactly as:

$$\min_{\mathbf{u}} \Phi(\mathbf{u}, \mathbf{d}) \quad (5a)$$

$$\text{s.t. } \mathbf{y}^L \leq \mathbf{y}(\mathbf{u}, \mathbf{d}) \leq \mathbf{y}^U, \quad (5b)$$

$$\mathbf{u}^L \leq \mathbf{u} \leq \mathbf{u}^U. \quad (5c)$$

For a defined disturbance value \mathbf{d} , the optimal operation point \mathbf{u}^* can be obtained by solving problem (5). In this sense, the optimal steady-state input is function of the process disturbance, i.e., $\mathbf{u}^*(\mathbf{d})$.

2.2. The closed loop control problem

Real processes are often affected by unmeasured or unknown disturbances and the presence of a plant-model mismatch. Therefore, a closed loop control structure is generally used in industrial plants in order to manipulate the input variables based on available measurable process variables.

These closed loop control structure can be represented by a set of equations and incorporated into the optimization problem (5). Consequently, we denote by \mathbf{y} to a vector that is constructed with the controlled output variables and the input variables that will remain fixed. The input variables that are not fixed in $\mathbf{r}(\mathbf{u}, \mathbf{y})$ are input variables used in the control loops as manipulated variables. We also introduce the vector $\mathbf{r}^{\text{sp}} \in \mathbb{R}^{n_u}$ that contains the set points values for the controlled variables and the fixed input variables.

Thus, the behavior of the controlled plant in steady-state can be defined by including the following n_u equations in the optimization problem:

$$\mathbf{r}(\mathbf{u}, \mathbf{y}(\mathbf{u}, \mathbf{d})) = \mathbf{r}^{\text{sp}}. \quad (6)$$

If we add Eq. (6) in problem 5 and a control structure is defined, then the set point values $\mathbf{r}^{\text{sp}} \in \mathbb{R}^{n_u}$ become now in the optimization variables of the mathematical programming problem.

2.3. The back-off as a self-optimizing control structure strategy

The objective of the back-off (BO) strategy for control structure selection is to define the fixed input values and the output set point values for the controlled and manipulated variables by minimizing the operation cost for a nominal disturbance (\mathbf{d}_n) while the constraints are guaranteed for the whole set of disturbances scenarios $\mathbf{d} \in \mathcal{D}$ [15]. On the other hand, the self-optimizing control (SOC) methods aim to select the controlled variables that minimize the expected value (or the weighted average value) of the economic loss for a given set of disturbances [16]. The economic loss is defined as the difference between the average operation cost that can be ideally achieved with the optimal mapping $\mathbf{u}^*(\mathbf{d})$ and the average operation cost obtained with the selected control structure.

In a recent work [17], the relationship between both strategies has been studied and a novel general approach for control structure selection has been proposed. Authors noticed that minimizing the average economic loss, as it is done in self-optimizing theory, is equivalent to minimize average cost. Therefore, if the back-off approach is forced to minimize the average cost (not only a nominal cost) the result is a back-off self-optimizing control structure problem.

A mathematical formulation for the control structure selection problem can be obtained by introducing in the vector of equations $\mathbf{r}(\mathbf{u}, \mathbf{y}) \in \mathbb{R}^{n_u}$ a vector of binary variables, \mathbf{z} , that determines the choice of control structure. Then Eq. (6) is modified as following:

$$\mathbf{r}(\mathbf{z}, \mathbf{u}, \mathbf{y}(\mathbf{u}, \mathbf{d})) = \mathbf{r}^{\text{sp}}. \quad (7)$$

Commonly in the literature on self-optimizing control, controlled variables are obtained by a linear combination of input and output variables. To represent these structures, denoted as lineal combination control structures, we can use the following expression:

$$\mathbf{r}(\mathcal{H}, \mathbf{u}, \mathbf{y}(\mathbf{u}, \mathbf{d})) = \mathcal{H}^T \begin{bmatrix} \mathbf{y}(\mathbf{u}, \mathbf{d}) \\ \mathbf{u} \end{bmatrix},$$

where $\mathcal{H} \in \mathbb{R}^{(n_u+n_y) \times n_u}$ is the matrix of linear combinations. Notice that the entries of the matrix \mathcal{H} (lineal combination control structure) are continuous variables, while the entries of the vector \mathbf{z} (classic control

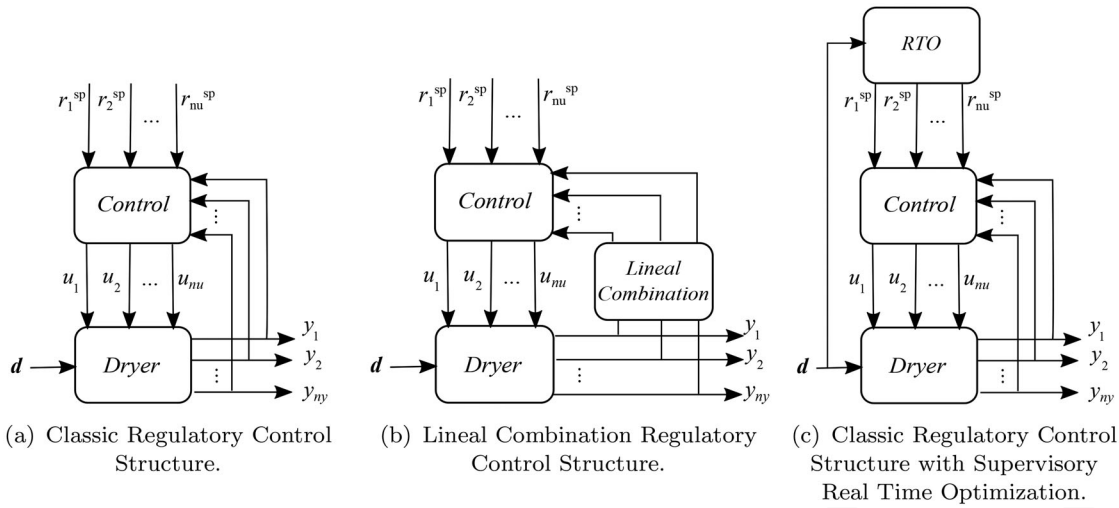


Figure 1. Alternatives control structures studied in this work. (a) Classic regulatory control structure. (b) Lineal combination regulatory control structure. (c) Classic regulatory control structure with supervisory real time optimization.

structure) are binary variables. Therefore the resulting mathematical formulations for the control structure selection are: a mixed-integer nonlinear programming problem (MINLP) for classic control structure, or a nonlinear programming problem (NLP) for the linear combination control structure.

2.4. The real-time optimization control layer

In highly automatized plants the control actions are usually separated into levels or layers. The first level is regulatory control. At this level, the objective is to keep the process operating in desired set point values and to reject unmeasured or fast disturbances. In a second level commonly a real-time optimization (RTO) control calculates the optimum steady-state operating point under changing conditions due to low-frequency or measurable disturbances and gives the optimum point to the regulatory control layer in the form of set points.

In order to incorporate the RTO action in the control structure selection problem we explicitly classify disturbances that affect the performance of the plant in the measurable disturbances $\hat{\mathbf{d}} \in \mathbb{R}^{n_a}$ and the unmeasurable disturbances $\tilde{\mathbf{d}} \in \mathbb{R}^{n_{\tilde{a}}}$. In the drying control process measurable disturbance information has typically been used for feed-forward control action, i.e., it is used to anticipate the impact of the disturbance in the process system. However, it is important to note that economic steady-state performance is not optimized by this classic feed-forward action approach [2]. In the work [19], authors studied the use of hierarchical control structure for grain dryers and showed the impact of grain moisture disturbance on the operation cost. Nevertheless, in that work,

a deterministic procedure for the selection of regulatory control structure closed loops is not considered, and controlled and manipulated variables were defined a priori.

Installing a real-time optimization control layer generally improves the economic performance of the process, however, as studied in [20] the optimal hierarchical control system would only be obtained if an integrated regulatory plus supervisory control structure selection problem is solved. This is because the optimization layer would attempt to change the set-points of the available control loops and the reference values for the fixed inputs. In other words, the optimization problem solved in the RTO block receives as constraints the regulatory control laws. Then, having installed regulatory control loops means constraints, and as a consequence, a particular optimization problem is solved for each regulatory control structure. Therefore, the optimal hierarchical control structure can be obtained if an integrated back-off self-optimizing plus RTO problem is solved [20]. With the proper disturbance classification $\mathbf{d} = [\hat{\mathbf{d}}; \tilde{\mathbf{d}}]$, we can take the RTO action into account in the control structure selection problem by using the following set point expression:

$$\mathbf{r}(\mathbf{z}, \mathbf{u}, \mathbf{y}(\mathbf{u}, \hat{\mathbf{d}}, \tilde{\mathbf{d}})) = \mathbf{r}^{\text{sp}}(\hat{\mathbf{d}}), \quad \forall [\hat{\mathbf{d}}; \tilde{\mathbf{d}}] \in \mathcal{D} \quad (9)$$

Figure 1 resumes the control strategies that will be studied in the present work for the drying process. While Figure 1a illustrates a classic regulatory control structure and Figure 1b uses a linear combination matrix to create virtual controlled variables, Figure 1c shows a hierarchical scheme with a RTO layer that aims to change the set point values of the control loops.

2.5. Additional constraints

A method for designing multiple-input multiple-output (MIMO) control structures is to find a diagonal or decentralized controller. In this way, the entire process can be viewed as a separable collection of sub-processes that can be independently designed. In this sense, the relative gain array (RGA) approach facilitates the design of a decentralized control system by analyzing control structure configurations with minimal interaction between the control loops. The RGA is a systematic tool used for the definition of input-output pairing in MIMO systems. In this paper, additional constraints are added to the optimization problem to achieve a decentralized control design. On one hand, for the classic control structures, we define the input-output pairing of the control loops based directly on the steady-state relative gain matrix (RGA). On the other hand, if a linear combination control structure is designed, the pairings are forced by imposing a well-conditioned matrix to the resulting controlled sub-process. In this work, we directly force a diagonal controller with the identity matrix. The additional constraints are given for the steady-state gain matrix obtained at the nominal optimal operation point, this is, for $\mathbf{u}^*(\mathbf{d}_n)$. Although this is not a sufficient controllability condition, it is useful to already exclude some control structures from the optimization problem. Once the optimal steady-state economic control structure is obtained, a dynamic study is necessary to validate the choice.

The equations for the RGA pairing are shown in Appendix A and a reformulation as a set of linear constraints can be found in [17].

3. Material and methods

In this section, we provide detailed information on the selected continuous dryer model, the proposed objective function, and constraints. A proper reformulation of the optimization problems for the selection of the control structure is also performed to use commercially available software and solvers.

3.1. Dryer model

There are several mathematical models in the bibliography based on the drying physics process and the drying technique [21, 22]. Considering also the dryer design parameters and the specific characteristics of the product to be dried, the amount of available models in the literature is extensive. Without loss of

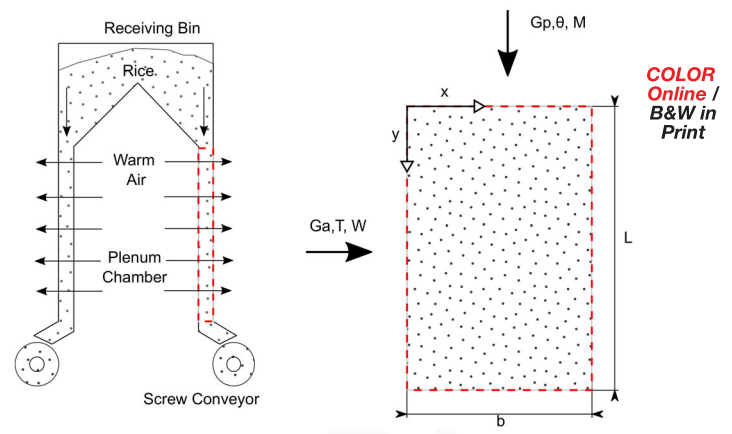


Figure 2. A cross-flow dryer and the simplified cross-section case study.

generality, in this work, we will use the mathematical model described in [23] for cross-flow dryers of rice grains. Although the control structure selection is made for the steady-state, a detailed dynamic model is necessary to perform a future validation and/or redesign of the obtained control structure. In this section, we will briefly present both equations and variables of the drying process, as well as the spatial discretization used in this work. A detailed description of the model can be found in [23].

A simplified cross-section of the dryer is shown in Figure 2. The air flows from the plenum chamber to outside the dryer while the grain flows from the top bin to the screw conveyor at bottom. The length and width of the drying section are denoted by L and b respectively. The coordinate along the latitudinal axis of the dryer is denoted by x and the coordinate along the longitudinal axis is denoted by y .

The corresponding model equations used in the optimization problem (1a, 1b, 1c) are:

- Material balance on the water in the grain:

$$-G_p \frac{\partial M}{\partial y} - \rho (1 - \epsilon) R = \rho (1 - \epsilon) \frac{\partial M}{\partial t}, \quad (10)$$

where G_p is the dry grain mass velocity in $[\text{kg}/\text{s}\cdot\text{m}^2]$, M is the moisture content of grain in $[\text{kg}/\text{kg}_{\text{drygrain}}]$, R is the drying rate in $[\text{kg}_{\text{water}}/\text{kg}_{\text{drygrain}}\cdot\text{s}]$, ρ is the density of dry grain in $[\text{kg}/\text{m}^3]$ and ϵ is the bed porosity in $[\text{m}^3_{\text{pores}}/\text{m}^3_{\text{totalvolume}}]$.

- Material balance on the water vapor in the air:

$$-G_a \frac{\partial W}{\partial x} + \rho (1 - \epsilon) R = \rho_a \epsilon \frac{\partial W}{\partial t}, \quad (11)$$

where G_a is the dry air mass velocity in $[\text{kg}/\text{s}\cdot\text{m}^2]$, W is absolute humidity of air in $[\text{kg}/\text{kg}_{\text{dryair}}]$ and ρ_a is the density of dry air in $[\text{kg}/\text{m}^3]$.

- **Energy balance on the grain:**

$$\begin{aligned}
 & -G_p C_{pg} \frac{\partial \theta}{\partial y} + h (T - \theta) \\
 & - \rho (1 - \epsilon) R (H_w - h_w) \\
 & = \rho (1 - \epsilon) C_{pg} \frac{\partial \theta}{\partial t}, \quad (12)
 \end{aligned}$$

where C_{pg} is the specific heat of wet grain in $[J/kg_{drygrain} \cdot ^\circ C]$, θ is the grain temperature in $[^\circ C]$, h is the volumetric convective heat transfer coefficient in $[J/m^3 \cdot s \cdot ^\circ C]$, T is the air temperature in $[^\circ C]$, h_w is the enthalpy of liquid water in $[J/kg]$ and H_w is the enthalpy of water vapor in $[J/kg]$.

- **Energy balance on the air phase:**

$$-G_a C_{pa} \frac{\partial T}{\partial x} - h (T - \theta) = \rho_a \epsilon C_{pa} \frac{\partial T}{\partial t}, \quad (13)$$

where C_{pa} is the specific heat of humid air in $[J/kg_{dryair} \cdot ^\circ C]$

- **Boundary conditions:** The partial differential equations (10–13) are subject to the following general boundary conditions:

$$W(0, y, t) = W_{in}(y, t), \quad (14)$$

$$T(0, y, t) = T_{in}(y, t), \quad (15)$$

$$M(x, 0, t) = M_{in}(x, t), \quad (16)$$

$$\theta(x, 0, t) = \theta_{in}(x, t), \quad (17)$$

In our case study we assume that the feed to the dryer is not a function of position, this is:

$$W(0, y, t) = W_{in}(t), \quad (18)$$

$$T(0, y, t) = T_{in}(t), \quad (19)$$

$$M(x, 0, t) = M_{in}(t), \quad (20)$$

$$\theta(x, 0, t) = \theta_{in}(t), \quad (21)$$

- **Initial conditions:** The initial conditions of the system equations are:

$$W(x, y, 0) = W_0(x, y), \quad (22)$$

$$T(x, y, 0) = T_0(x, y), \quad (23)$$

$$M(x, y, 0) = M_0(x, y), \quad (24)$$

$$\theta(x, y, 0) = \theta_0(x, y). \quad (25)$$

- **Rate of drying (empirical relations for rice):**

$$\begin{aligned}
 R &= 10^{-5} (4.6889 + 0.10558 (T + \theta) \\
 &- 4.3667 rh) (M - Me) \quad (26)
 \end{aligned}$$

where Me is the equilibrium moisture content, and rh is the relative humidity of the air. The equilibrium moisture content is given by:

$$Me = E - F \times \ln(-(T + G) \times \ln(rh)) \quad (27)$$

where, for rough rice, the following coefficients are used: $E = 0.29394$, $F = 0.046015$ and $G = 35.703$. The relative humidity of the air, rh , is given by:

$$rh = 1.01325 \times 10^5 \times WMa / (WMa + Mw)Pv \quad (28)$$

where Ma is the molecular weight of air, Mw is the molecular weight of water, in this work 28.9647 and 18.0153 $[kg/kmole]$ respectively. The vapor pressure of water Pv at temperature T is obtained through the Antoine's equation:

$$\log_{10}(Pv) = 8.07131 - (1730.63 / (T + 233.426)) \quad (29)$$

- **Convective heat transfer coefficient (empirical relation for rice):** The correlation for volumetric convective heat transfer coefficient in a packed bed of rice:

$$h = 8.69 \times 10^4 G_a^{1.3} \quad (30)$$

- **Input Mass Velocity:** For our case we assume that the input mass velocity G_a and G_p depend on time only:

$$G_a = G_a(t) \quad (31)$$

$$G_p = G_p(t) \quad (32)$$

The spatial derivatives are discretized by using a finite difference approach. The cross-section dryer is then divided into N_r rows and N_c columns as shown in Figure 3. Using the line method, the four process equations (10–13) lead to $4 \times N_r \times N_c$ coupled ODES that are added to the mathematical optimization problem. The choice of N_r and N_c for the present model is also discussed in [23]. In this work, we use a 4×4 discretization.

Moreover, in this work, we use a scaled version of the model as was presented in the work [23]. We scale the model based on the economic optimal operation point at the nominal disturbance scenario, this is, $\mathbf{u}^*(\mathbf{d}_n)$. Calculations for scaled versions of process variables can be found in the B. Finally, in Table 1 the dryer parameters are listed.

3.2. Process variables and constraints

A first step in the study of control structures is to identify the available manipulable input variables (\mathbf{u}), the measurable output variables (\mathbf{y}), and the disturbances (\mathbf{d}) of the dryer [1]. A second step is the

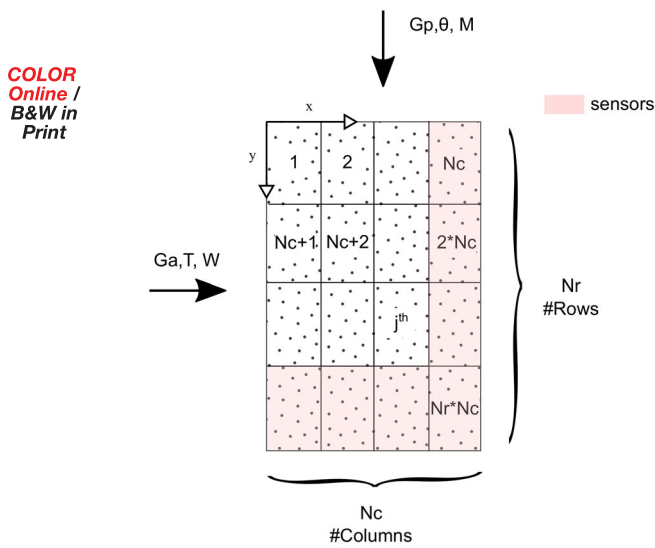


Figure 3. Discretization of the cross-section dryer.

Table 1. Dryer parameters.

Process Parameters	Case Study	Dimension	Value
Dryer length	L	[m]	21.30
Dryer width	b	[m]	0.28
Bed porosity	ϵ	$[m^3_{pores}/m^3_{total\ volume}]$	0.57
Density of dry air	ρ_a	$[kg/m^3]$	1.13
Density of dry grain	ρ	$[kg/m^3]$	1394
Specific heat of humid air	C_{pa}	$[J/kg_{dry\ air} \cdot ^\circ C]$	1005
Specific heat of wet grain	C_{pg}	$[J/kg_{dry\ grain} \cdot ^\circ C]$	2094

definition of the constraints on the process operation. In general, these constraints vary depending on the case study, type of dryer and product, ambient conditions, etc. While manipulated variables are usually constrained by dryer design and/or production requirements, the limits on output variables are given by product quality and safe operation. Also, disturbance constraints are commonly obtained based on historical data.

In this work, the continuous cross-flow grain dryer model proposed by [24] is used. In this sense, the design dryer parameters, length, and cross-section of the dryer are fixed. Additionally, in this model, the air temperature and the air mass velocity need to be bounded to guarantee certain empirical relations, e.g., the volumetric convective heat transfer coefficient. The grain temperature and the grain mass velocity are also constrained to guarantee the quantity and quality of the output product.

For this dryer model and for the considered scenarios, it is not feasible to reduce the output moisture to the commonly safe value of 14%. In order to keep a valid and useful case study model we upper bound the output moisture in 19% which is near the average nominal output moisture solution obtained in [24]. In this way, the approach applied to the constrained case

study analyzes the economic performance of the dryer model based on available data.

The main variables and constraints considered in the present work are shown in Table 2.

3.3. Functional cost

This work aims to find control structures that minimize the operating cost per unit of dried grain. In this sense, the operation cost includes the fuel cost to raise the inlet air temperature to the desired value and the electric cost associated with the air blowing fan. In [6] some additional terms are also considered in the functional cost, such as the cost associated with the output moisture content and the cost of quality loss due to thermal damage. However, these costs are not taken into account in this work, since the moisture content and the product quality are guaranteed by a set of constraints into the optimization problem. It is important to note that the dry grain mass velocity is a manipulated variable in our optimization problem. Therefore, if we need to produce a predefined quantity of dry grains, we only have to adjust (or set) this variable using the appropriate upper and lower bounds proposed in the optimization problem.

3.3.1. Fuel cost

Like in the work of [6], we consider a cost associated to air heating as follows:

$$C_{f_{top}} = t_{op} P_f G_a (L a) \frac{C_{pa}}{Z_f} (T_{in} - T_{amb}) \quad (33)$$

where t_{op} is the operation time in [s], P_f is the cost of fuel in [\$/l], Z_f is its calorific power in [J/l] and $(L a)$ is the dryer area in $[m^2]$. The values used in this work are: $P_f = 1$, $Z_f = 3.6 \times 10^7$ and $T_{amb} = 25$.

3.3.2. Operation cost of electric fan

We also consider the electricity cost associated with the air fan. For this purpose, we approximate the power consumption based on the system airflow resistance and the fan operation using a variable frequency drive, see Figure 4.

First, we need to estimate the pressure drop curve of the system, in our case, it will be based on the model information. In [25] the airflow resistance for a rice deep bed are studied considering different moisture, fines, bulk density, and air velocities. The author approximated the system curve as follows:

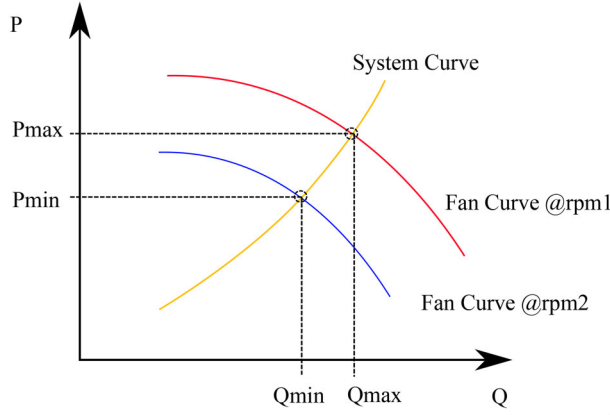
$$P = V_a (b_1 F + b_2 MC + b_3 BD + b_4 V_a) \quad (34)$$

where $b_1 = 25.859$, $b_2 = -90.056$, $b_3 = 5.587$, and $b_4 = 9133.696$ are regression coefficients, P is the

Table 2. Process variables and constraints (steady-state).

Process Variable	Type	Case Study	Dimension	Constraint	
				Lower Bound	Upper Bound
Inlet Air Temperature	u	T_{in}	[°C]	45	65
Dry Air Mass Velocity	u	G_a	[kg/s.m ²]	0.25	0.55
Dry Grain Mass Velocity	u	G_p	[kg/s.m ²]	2	12
Outlet Air Temperature	y	T_{out}	[°C]	—	—
Outlet Absolute Humidity of Air	y	W_{out}	[kg/kg _{dryair}]	—	—
Outlet Grain Temperature	y	θ_{out}	[°C]	—	60
Outlet Moisture Content of Grain	y	y	[kg/kg _{drygrain}]	—	0.19
Inlet Absolute Humidity of Air	d	W_{in}	[kg/kg _{dryair}]	0.006	0.012
Inlet Grain Temperature	d	θ_{in}	[°C]	25	35
Inlet Moisture Content of Grain	d	M_{in}	[kg/kg _{drygrain}]	0.20	0.25

COLOR
Online /
B&W in
Print

**Figure 4.** Operation point based on the airflow resistance system curve and using a variable frequency drive control for the fan.

pressure drop in [Pa/m], V_a is the air velocity in [m/s], F is the fines percentage [%], MC is the moisture content [%Wb] and BD is the bulk density in [kg/m³].

For simplicity let's consider constant $MC = 20\%$, $F = 0$ and $BD = 599.42 = \rho (1 - \epsilon)$, then Eq. (34) for our dryer model (with a rice deep bed $b = 0.28$ [m]) is reduced to:

$$P_b = V_a (433 + 2557 V_a), \quad (35)$$

Substituting $V_a = \frac{G_a}{\rho_a}$:

$$P_b = \frac{G_a}{\rho_a} \left(433 + 2557 \frac{G_a}{\rho_a} \right), \quad (36)$$

and the power consumption in [kW] is given by:

$$W = \frac{P_b Q_a}{1000 \eta}, \quad (37)$$

where η is the fan efficiency (in this work 0.5) and Q_a is the volumetric flow rate in [m³/s] obtained by $Q_a = G_a L a / \rho_a$. Finally, considering the operation time t_{op} [s] and the price of energy P_e [[\$]/kWh] (in this work 0.1), the operative cost of the fan is obtained as follows:

$$C_{etop} = \frac{t_{op} P_e W}{3600} \quad (38)$$

3.3.3. Total unitary cost

As mentioned before, in this work we propose to minimize the operation cost per unit of dried grain [[\$]/ton]. Taking into account the fuel cost (C_{ftop}) and electricity cost associated with the air fan (C_{etop}) the objective function can be formulated as follow:

$$J = 1000 \frac{C_{ftop} + C_{etop}}{t_{op} G_p a b} \quad (39)$$

From 33 and 38 the objective function J of 39 would be minimized if we can operate at higher G_p with reduced G_a and T_{in} . Considering the operation and quality constraints for the several disturbance scenarios, the optimal control structure and their set point values need to be obtained by the proper formulation of constrained optimization problems.

3.4. Problem formulation

In this section, a detailed description of the control structure selection problems presented in the previous sections (2.3, 2.4) for the drying process model is shown. Based on the case study variables and constraints presented in Table 2 and for the spatial discretized dryer model ($N_r = 4$, $N_c = 4$), we define the following variables:

$$\mathbf{u} = [G_a, G_p, T_{in}], \quad (40)$$

$$\mathbf{y} = [W_4, W_8, W_{12}, W_{16}, T_4, T_8, T_{12}, T_{16}, M_{13}, M_{14}, M_{15}, M_{16}, \theta_{13}, \theta_{14}, \theta_{15}, \theta_{16}], \quad (41)$$

$$\mathbf{d} = [W_{in}, \theta_{in}, M_{in}], \quad (42)$$

where \mathbf{u} is the vector of input variables with dimension $n_u = 3$, \mathbf{y} is the vector measurable output variables with dimension $n_y = 16$, and \mathbf{d} is the vector of disturbance variables with dimension $n_d = 3$. It is

important to highlight that the j -th index used for measurable output variables refers to each compartment associated with the $N_r \times N_c$ discretization (see Figure 3), i.e., we are measuring temperature and moisture variables at the compartments nearby to the dryer output.

3.4.1. Classic back-off self-optimizing control structure

The classic control structure selection is formulated by the following parametrization:

$$\mathbf{z} = \begin{bmatrix} \mathbf{z}^O \\ \mathbf{z}^I \end{bmatrix}, \quad \mathbf{z}^O \in \mathbb{B}^{n_y}, \quad \mathbf{z}^I \in \mathbb{B}^{n_u}, \quad (43)$$

$$\mathbf{r}^{sp} = \begin{bmatrix} \mathbf{y}^{sp} \\ \mathbf{u}^{sp} \end{bmatrix}, \quad \mathbf{y}^{sp} \in \mathbb{R}^{n_y}, \quad \mathbf{u}^{sp} \in \mathbb{R}^{n_u}. \quad (44)$$

The entries in the vector \mathbf{z}^I with unitary value indicate the input variables that remain fixed, i.e., inputs not used for the control. Similarly, binary entries with values equal to one in the vector \mathbf{z}^O indicates the output variables selected to be controlled (CV). On the other hand, the entries in \mathbf{y}^{sp} and \mathbf{u}^{sp} give the set point values for controlled and fixed input variables, respectively. To solve the control structure selection problem, we approximate the process disturbance region by a finite number of possible scenarios. We use a uniform mesh where discrete disturbances are considered, i.e., $d_1 = W_{in} \in \{0.006, 0.009, 0.012\}$, $d_2 = \theta_{in} \in \{25, 30, 35\}$ and $d_3 = M_{in} \in \{0.2, 0.23, 0.25\}$. This lead to a discrete set of disturbance scenarios $\underline{\mathcal{D}}$, with $N=27$ possible realization of \mathbf{d} . The nominal disturbance scenario is selected as $\mathbf{d}_n = [0.009, 35, 0.23]$. Additionally, the following sets are defined:

$$\mathcal{U} = \{1, 2, n_u = 3\}, \quad \mathcal{Y} = \{1, 2, \dots, n_y = 16\},$$

$$\mathcal{K} = \{1, 2, \dots, N = 27\}.$$

Finally, the back-of self-optimizing classic control structure selection can be formulated as follows:

$$\min_{\mathbf{z}, \mathbf{r}^{sp}} \sum_{k=1}^N p_k J(\mathbf{u}_k, \mathbf{d}_k) \quad (45a)$$

$$\text{s.t. steady-state model equations } \forall \mathbf{k} \in \mathcal{K}, \quad (45b)$$

$$\sum_{i=1}^{n_y} z_i^O + \sum_{j=1}^{n_u} z_j^I = n_u, \quad (45c)$$

$$\sum_{i=1}^{n_y} z_i^O \leq n_{loops}, \quad (45d)$$

$$\text{RGA pairing equations for } \mathbf{d} = \mathbf{d}_n, \quad (45e)$$

$$y_i^L z_i^O \leq y_i^{sp} \leq y_i^U z_i^O, \forall i \in \mathcal{Y}, \quad (45f)$$

$$u_j^L z_j^I \leq u_j^{sp} \leq u_j^U z_j^I, \forall j \in \mathcal{U}, \quad (45g)$$

$$y_i^L (1 - z_i^O) \leq y_i(\mathbf{u}_k, \mathbf{d}_k) - y_i^{sp} \leq y_i^U (1 - z_i^O), \forall i \in \mathcal{Y}, k \in \mathcal{K}, \quad (45h)$$

$$u_j^L (1 - z_j^I) \leq u_{j,k} - u_j^{sp} \leq u_j^U (1 - z_j^I), \forall j \in \mathcal{U}, k \in \mathcal{K}, \quad (45i)$$

The objective function (45a) is a weighted sum of the total cost (39) over the specified set of disturbance scenarios. The parameters p_k are the weights for each disturbance scenario, in our study case we use $p_k = \frac{1}{N}$, $\forall k$. The set of equations (45b) are the dryer model equations in steady-state that must be solved for all the set of disturbance scenarios. For our case study this means the material and energy balance equations, Eqs. (10)–(13), the drying rate equation, Eq. (26), convective heat transfer, Eq. (30), and initial and boundary conditions, Eqs. (14)–(25). It is important to highlight that model equations are considered for each discrete dryer compartment (i.e., for $N_r \times N_c$ compartments) and, also, for all scenarios of possible disturbances (i.e., N scenarios). On the other hand, while Eq. (45c) states that the total number of fixed variables must be equal to the total number of input variables and Eq. (45d) defines the maximal number of control loops, the set of equations (45e) is given to perform the input-output pairing for the selected controlled loops based on RGA steady-state matrix evaluated at the nominal optimum $\mathbf{u}^*(\mathbf{d}_n)$. In this formulation, if output and input variables are selected as controlled and manipulated variables, their set points have to be within the upper and lower bounds, Eqs. (45f) and (45g), otherwise, they are set to zero. By Eqs. (45h) and (45i) the controlled output variables and fixed input variables of the control structure selected are forced to follow their set point value for all disturbance scenarios $\mathbf{d}_k \in \underline{\mathcal{D}}$. The remaining variables that do not belong to the control structure are restricted to their upper and lower bound for all disturbance scenarios $\mathbf{d}_k \in \underline{\mathcal{D}}$.

3.4.2. Linear combination back-off self-optimizing control structure

In this section, we use the linear combination matrix $\mathcal{H} \in \mathbb{R}^{(n_u+n_y) \times n_u}$ to define the control structure and the discrete set of disturbance scenarios $\underline{\mathcal{D}}$. Therefore, the problem for optimal control structure selection can be formulated as follows:

983
984
985
986
987
988
989
990
991
992
993
994
995
996
997
998
999
1000
1001
1002
1003
1004
1005
1006
1007
1008
1009
1010
1011
1012
1013
1014
1015
1016
1017
1018
1019
1020
1021
1022
1023
1024
1025
1026
1027
1028
1029
1030
1031
1032
1033
1034
1035
1036
1037
1038
1039
1040

$$\min_{\mathcal{H}, \mathbf{r}^{\text{sp}}} \sum_{k=1}^N p_k J(\mathbf{u}_k, \mathbf{d}_k) \quad (46a)$$

$$\text{s.t. } \text{steady-state model equations } \forall k \in \mathcal{K}, \quad (46b)$$

$$\mathcal{H}^T \begin{bmatrix} \mathbf{y}(\mathbf{u}_k, \mathbf{d}_k), \\ \mathbf{u}_k \end{bmatrix} = \mathbf{r}^{\text{sp}}, \quad (46c)$$

$$\forall k \in \mathcal{K}, \mathcal{H}^T \begin{bmatrix} \mathbf{G} \\ \mathbf{I} \end{bmatrix} = \mathbf{T}, \quad (46d)$$

$$\mathbf{y}^L \leq \mathbf{y}(\mathbf{u}_k, \mathbf{d}_k) \leq \mathbf{y}^U, \forall k \in \mathcal{K}, \quad (46e)$$

$$\mathbf{u}^L \leq \mathbf{u}_k \leq \mathbf{u}^U, \forall k \in \mathcal{K}. \quad (46f)$$

where, in Eq. (46d), $\mathbf{G} \in \mathbb{R}^{n_y \times n_u}$ is the input-output gain matrix of the open-loop system, evaluated at the nominal optimum $\mathbf{u}^*(\mathbf{d}_n)$, and $\mathbf{T} \in \mathbb{R}^{n_u \times n_u}$ is the gain matrix imposed on the controlled process (in general, any well-conditioned matrix). Note that the choice of \mathbf{T} will also determine the pairing of manipulated variables with controlled variables.

3.4.3. Back-off self-optimizing plus real-time optimization

In order to incorporate the RTO layer, we first have to partition the set of disturbance scenarios. We introduce the measurable disturbance index set:

$$Q = \{1, 2, \dots, N_q\},$$

Therefore, the total disturbance scenarios are now defined by $N = N_q \times N_k$. For example, if the inlet grain moisture, M_{in} , can be measurable, then we can rearrange the set of $N = 27$ disturbances as a 3×9 set as is shown in Table 3.

Then it is possible to reformulate the equations of problem 45 by evaluating them at $(\mathbf{u}_{q,k}, \mathbf{d}_q, \mathbf{d}_k)$ and replacing the fixed set points strategy with a variable set points strategy.

In problem 45, replace the set point equations (45f)–(45i) by:

$$y_i^L z_i^O \leq y_{i,q}^{\text{sp}} \leq y_i^U z_i^O, \forall i \in \mathcal{Y}, q \in Q, \quad (47a)$$

$$u_j^L z_j^I \leq u_{j,q}^{\text{sp}} \leq u_j^U z_j^I, \forall j \in \mathcal{U}, q \in Q, \quad (47b)$$

$$y_i^L (1 - z_i^O) \leq y_i(\mathbf{u}_{q,k}, \mathbf{d}_{q,k}) - y_{i,q}^{\text{sp}} \leq y_i^U (1 - z_i^O), \\ \forall i \in \mathcal{Y}, k \in \mathcal{K}, q \in Q, \quad (47c)$$

Table 3. Disturbance scenario discretization ($d = [\hat{d}; \tilde{d}]$).

	q1				q2				q3			
	k1	k2	...	k9	k1	k2	...	k9	k1	k2	...	k9
M_{in}	0.2	0.2	...	0.2	0.23	0.23	...	0.23	0.25	0.25	...	0.25
W_{in}	0.006	0.009	...	0.012	0.006	0.009	...	0.012	0.006	0.009	...	0.012
θ_{in}	25	25	...	35	25	25	...	35	25	25	...	35

$$u_j^L (1 - z_j^I) \leq u_{j,q,k} - u_{j,q}^{\text{sp}} \leq u_j^U (1 - z_j^I), \forall j \in \mathcal{U}, k \in \mathcal{K}, q \in Q, \quad (47d)$$

4. Simulation results

In this section, we study a variety of back-off self-optimizing control structures strategies in order to evaluate which is the best option based on steady-state economic criteria. The mathematical programming problems presented in Section 3.4 are implemented in GAMS v37.1.0 environment. All study cases are solved on an AMD Ryzen 7 3700 × 8-Core Processor @3.59 GHz with 16 gb ram.

4.1. Optimal operation and open loop structure

Initially, we are going to solve the problem 5 for all discrete disturbance scenarios in order to find the minimal bound for the operation cost (J_{opt}). Using this procedure, we can obtain the optimal values of manipulated variables $\mathbf{u}^*(\mathbf{d})$ and determine if there are input or output variables that remain active for the whole set of perturbations. Recall that optimal mapping $\mathbf{u}^*(\mathbf{d})$ is an idealized condition that requires perfect knowledge of the disturbance values, therefore both J_{opt} and $\mathbf{u}^*(\mathbf{d})$ are used as references. Secondly, we are going to calculate (if possible) the cost associated with an open loop strategy (J_{ol}). To obtain the solution to this open loop strategy, we solve problem 45 by fixing all available manipulated variables, i.e., all components of binary variable \mathbf{z}^I are set equal to one.

Hence, we obtain that the optimal operating cost (lower operation cost bound) is an average value of $J_{opt} = 5.236$ [[\$]/ton] and the output variable M_{16} is always active at the upper bound ($M_{16} = 0.19$) for all considered scenarios. On the other hand, we found that it is possible to set an open loop strategy that remains feasible for all disturbances scenarios by fixing the manipulated variables to the following set points: $G_a = 0.31$, $G_p = 2$, $T_{in} = 55$. The associated operation cost for the open loop strategy is $J_{ol} = 10.05$.

This work attempts to bring self-optimizing control (SOC) approaches to grain drying processes. As mentioned in Section 2.3, the idea behind self-optimizing control is to find the control structure that automatically leads to the optimal movements of the manipulated variables, $\mathbf{u}^*(\mathbf{d})$, and, with it, to the optimal operating conditions, J_{opt} . In this sense, the SOC approach minimizes the difference between an average

operation cost of the controlled process, J_{cs} , and an ideal optimal average operation cost, J_{opt} . This objective function is defined as the optimality loss and it is useful to compare the performance of different control structures (and find the best solution).

The optimality loss for a given control structure (represented by the subscript cs) can be obtained as follows:

$$Loss_{cs} = (J_{cs} - J_{opt}), \quad (48)$$

The optimization loss can also be expressed in a percentile as follows:

$$Loss_{cs}[\%] = 100 \frac{(J_{cs} - J_{opt})}{J_{opt}}, \quad (49)$$

Then, the optimality loss for the open loop structure has a value of 91.90[%].

4.2. Classic closed loop control structure

In this section, we propose to solve two alternative control structures. The case (A) where all the output variables presented in 3.4 are available to measure and also a case (B) where the output grain moisture is not available for control purpose. The aim of case (B) is to contemplate industrial-drying plants where moisture sensors are not available since they are expensive or have low reliability [1]. Therefore, the vector y of output measurable variables are:

$$y_A = [W_4, W_8, W_{12}, W_{16}, T_4, T_8, T_{12}, T_{16}, M_{13}, M_{14}, M_{15}, M_{16}, \theta_{13}, \theta_{14}, \theta_{15}, \theta_{16}], \quad (50)$$

$$y_B = [W_4, W_8, W_{12}, W_{16}, T_4, T_8, T_{12}, T_{16}, \theta_{13}, \theta_{14}, \theta_{15}, \theta_{16}] \quad (51)$$

The obtained optimal solution for case (A) is to control $M_{16} = 0.19$ using the manipulated variable G_p and to fix the input variables G_a and T_{in} in an optimal set point values ($G_a = 0.344$; $T_{in} = 51.92$). The optimization loss is reduced to a 14.24%. Although the operation is still far from the optimal lower bound, the economic improvement respect to the open loop is already high. Case (B), gives the optimal solution of controlling $\theta_{16} = 42.03$ and also fixing $G_a = 0.29$ and $T_{in} = 62.5$, however, the solution still has an important optimality loss of 65.99%.

As mentioned in the introduction section, the selection of the control structure directly impacts the process operation and as consequence the economic performance. Case (B) closed-loop is a clear example

of this. The obtained structure achieves poor economic results when trying to satisfy the operation constraints, for the whole set of disturbance scenarios and with fixed set points.

The closed-loop case (A) and case (B) both fix G_a and T_{in} , but the set point values are different, then the impact of these variables in the functional cost differs. The remaining control loop uses G_p as manipulated variable for both structures. However, the movement of this variable is also different and impact in operation cost.

Case (A) aims to keep grain moisture output $M_{16} = 0.19$, this is an expected result as this constraint is founded always active in the ideal optimal operating conditions. The movements of manipulated variable G_p keep the (minimal) required output moisture for all the disturbance scenarios. The fixed values for G_a and T_{in} together with the movements of G_p are optimized to achieve the best average operation cost.

Case (B) aims to keep a fixed grain temperature output value. This control structure needs to find a set point for θ_{16} , and the fixed values for G_a and T_{in} , that can accomplish (at least) the output moisture of %19 while the operation cost is also minimized for the whole set of disturbance scenarios. This is not a simple and trivial task. The optimization problem finds that the best solution is to keep $\theta_{16} = 42.026$, $G_a = 0.29$ and $T_{in} = 62.5$. Analyzing the obtained results we observed that variable M_{16} : (a) only reaches the minimal output moisture of %19 in one disturbance scenario (worst case), (b) is near %18.5 in a few scenarios, and (c) is much less than %19, i.e., the grain is over dried, in the rest of the scenarios. The control loop is just looking to keep the output temperature of the grain in the defined set point, no matter if a favorable scenario occurs (for example a lower grain input moisture together with a lower air humidity). This means unnecessary higher operation costs or, as in SOC literature, a loss of optimality.

The complete steady-state values for input and output variables can be found in [supplementary information](#). Table 4 synthesize the findings for best classical control structure.

Table 4. The classic closed loop BO-SOC control structure selection problem.

	Selected Variables	Average Cost [\$/ton]	Optimal Loss [%]
Case A	M_{16}, G_a, T_{in}	5.982	14.24
Case B	θ_{16}, G_a, T_{in}	8.692	65.99

4.3. Lineal combination closed loop control structure

In this section, we present the result of using the lineal combination matrix for control structures. We are also going to consider a case (A) where all the output variables presented in 3.4 are available to measure and the case (B) where the output grain moisture is not available for control purpose.

For case (A) we look first for the economic lower bound that can be achieved by using all the available measurable variables (inputs and outputs). The result is an almost optimal operation with an average cost of $J = 5.259 [\$ / ton]$ (this is an optimal loss of only 0.43%). Then, we progressively decrease the quantity of output measured variables and re-calculate the optimal coefficients for the combination matrix and set point values. The study considers linear combination control structures by measuring 7, 11, 15, and 19 (all) variables. For case (B) we can do a similar analysis by considering sets of 7, 11 and 15 variables.

The coefficients obtained for lineal combination matrices are reported in [supplementary material](#) associated with this article. The resulting average costs and associated losses can be observed in [Table 5](#). The improvement in optimality loss is progressive as we consider more variables for the lineal combination matrix, and for the same quantity of variables, case (A) is always better than case (B). A tradeoff between the economic performance and the complexity of the resulting linear combination control structure (dynamic response, controller installation, operation, and maintenance) has to be considered before taking a decision. In this sense, is recommended to study the economic performance of alternatives to the full lineal combination matrix (which combines all available measurable variables).

The case (B) shows some interesting results as the optimality loss can be reduced considerably despite the absence of online output grain moisture sensors. The classic control structure solution for case (B) is a 65.99% of optimality loss ([Table 4](#)) and with a lineal combination control structure strategy the optimality loss is reduced to 0.82 %.

Table 5. The combination matrix closed loop BO-SOC control structure selection problem.

	Qty Variables	Average Cost [\$/ton]	Optimal Loss [%]
Case A	7	5.467	4.40
	11	5.282	0.88
	15	5.261	0.48
	19	5.259	0.42
Case B	7	5.606	7.06
	11	5.324	1.67
	15	5.279	0.82

4.4. Classic control structure plus real-time optimization

In this final section, we propose to use a hierarchical control structure with a real-time optimization layer. The main objective is to find the best regulatory control structure for the two layer control system. The analysis is again divided into case (A) and case (B). For both studies, we run the optimal classic BO-SOC + RTO control structure selection problem 45 with set point strategy 47 and compare the potential economic performance of the system by measuring inlet grain moisture versus inlet grain temperature or inlet air humidity. When the measurable disturbances enter the process the real-time optimization layer recalculates the set points in order to achieve an optimal economic performance (without violating process constraints for the rest of the unmeasured disturbance scenarios). The different strategies with the resulting average costs and optimality losses are presented in [Table 6](#) and the complete report with set points values can be found in [supplementary material](#).

For case (A), where all output variables can be measured, the best regulatory control layer for applying a hierarchical structure is again a unique closed-loop $M_{16} - G_p$ (together with optimal reference values for G_a and T_{in}). Also, from [Table 6](#), we can observe that effort in measuring the inlet grain temperature or inlet air humidity lead to an improvement that is not such as significant as the improvement obtained by measuring the inlet grain moisture.

For case (B), the best regulatory control layer for the hierarchical strategy depends on the available measured disturbance. In this case the economic improvement compared with only a regulatory layer (see [Table 4](#)) is considerable when measuring inlet grain moisture disturbance or inlet air humidity, reducing the optimality loss from a 65.99% to a 18.52% or 16.77% respectively. Notice also that in case (B) the optimal control structure obtained for a single regulatory layer strategy ([Table 4](#)) is not the best structure for the use of a RTO hierarchical strategy.

5. Discussion

In [Figure 5](#), the optimality loss versus the proposed control structure strategies for both cases (A-B) is resumed. Based on our findings, we provide the following recommendations:

- Open Loop and Classic Closed Loop Control Structures: The use of an open loop control structure operation is far from a good option. The

Table 6. Measurable disturbance and hierarchical control structure economic performance.

	Measured Disturbance	Selected Variables	Average Cost [\$/ton]	Optimal Loss [%]
Case A	θ_{in}	M_{16}, G_a, T_{in}	5.883	12.35
	W_{in}	M_{16}, G_a, T_{in}	5.701	8.87
	M_{in}	M_{16}, G_a, T_{in}	5.467	4.41
Case B	θ_{in}	T_8, θ_{13}, T_{in}	8.173	56.08
	W_{in}	W_{12}, T_{12}, G_a	6.114	16.77
	M_{in}	G_p, G_a, T_{in}	6.206	18.52

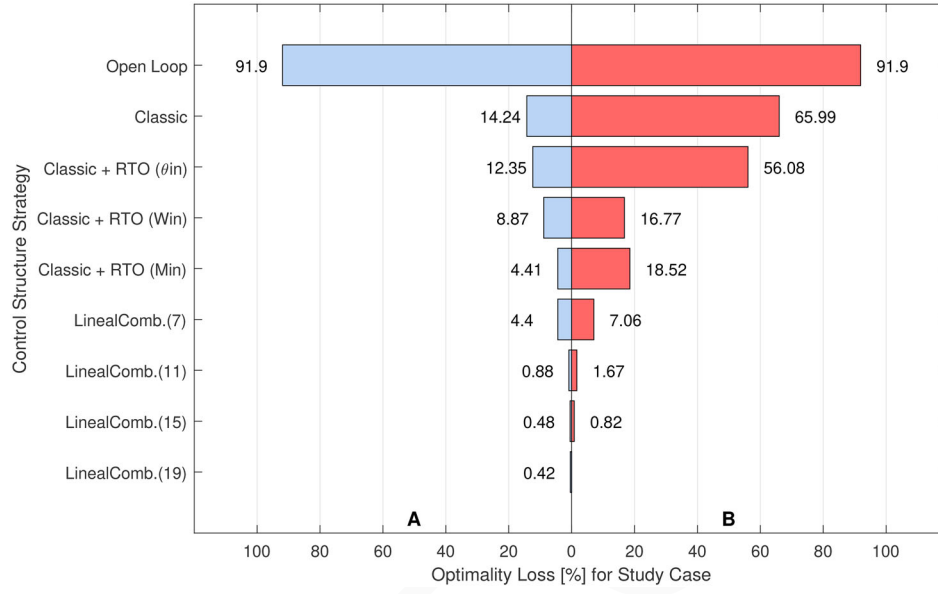


Figure 5. A comparison of the average optimality loss for the different control structure strategies. In case (a) all the output variables are available to measure and in case, (b) the output grain moisture is not available for control purpose.

traditional structure $M_{16} - G_p$ for continuous cross-flow dryers is proved to be the best regulatory classic closed loop structure from an economic steady-state point of view, notice although that the proper set points values for G_a and T_{in} for wide disturbances scenarios must be obtained from optimization. A classic output grain temperature closed loop ($\theta_{16} - G_p$) is confirmed to be highly sub-optimal.

- Lineal Combination Matrix for Closed Loop Control Structures: As we successively add measurable variables to the combination matrix the closed loop control strategy improves the steady-state economic performance (for both cases A-B), however a tradeoff between practical implementation and economic improvement must be considered. In the absence of online grain moisture sensors, a control strategy with a linear combination matrix of temperature and air humidity variables significantly improves the economic performance.
- Real-Time Optimization: The installation of a hierarchical control structure is a great opportunity for a continuous cross-flow grain drying process. For the studied case, a real-time optimization based on inlet grain moisture and the classic ($M_{16} - G_p$)

closed loop has shown good economic performance. As the feedback control loop ($M_{16} - G_p$) is used in industrial dryers and the inlet moisture is also suggested to measure for a feed-forward control strategy, it seems to be straightforward the implementation of a real-time optimization layer in order to improve the economic performance of grain dryers.

6. Conclusions

The results show that the selection of an adequate control structure and set point values has a significant economic impact on the drying process operation. For the study case, the operation of drying process in an open loop strategy is nearly 92% more expensive than an ideal optimal operation. In the case where output grain moisture sensors are available the obtained control structure and set point values significantly reduce the operation cost to an average optimality loss of 14%. Furthermore, the proposed strategies with virtual controllable variables is shown to improve economic performance, even if grain moisture sensors are not available (in the range of 7% to 0.4% of optimality loss depending on the control structure). Also, the use

COLOR Online / B&W in Print

1389
1390
1391
1392
1393
1394
1395
1396
1397
1398
1399
1400
1401
1402
1403
1404
1405
1406
1407
1408
1409
1410
1411
1412
1413
1414
1415
1416
1417
1418
1419
1420
1421
1422
1423
1424
1425
1426
1427
1428
1429
1430
1431
1432
1433
1434
1435
1436
1437
1438
1439
1440
1441
1442
1443
1444
1445
1446

1447
1448
1449
1450
1451
1452
1453
1454
1455
1456
1457
1458
1459
1460
1461
1462
1463
1464
1465
1466
1467
1468
1469
1470
1471
1472
1473
1474
1475
1476
1477
1478
1479
1480
1481
1482
1483
1484
1485
1486
1487
1488
1489
1490
1491
1492
1493
1494
1495
1496
1497
1498
1499
1500
1501
1502
1503
1504

of a hierarchical system with a real-time optimization layer based on inlet grain moisture it is a great opportunity for improvement.

The presented formulation for control structure selection is a useful tool for economics analysis and decision-making. The implementation of automatic process control strategies, online sensors investment, and intelligent control systems development for the study case is economically justified.

Finally, it is worth mentioning that although the work focuses on the search for an optimal control system for continuous cross-flow grain dryers, it is also possible and advisable to apply the methodology to diverse products and dryer technologies.

Future research directions may consider the dynamics response of the dryer for the proposed control structures and an in deep study of the real-time control layer for the case where a mismatch between the model and the plant is present.

Disclosure statement

No potential conflict of interest was reported by the author(s).

Funding

The authors thank the financial support from Pontificia Universidad Católica Argentina (UCA), Consejo Nacional de Investigaciones Científicas y Técnicas (CONICET), and Centro Franco-Argentino de Ciencias de la Información y de Sistemas (CIFASIS).

References

- Q1 [1] Jumah, R.; Mujumdar, A.; Raghavan, V. *Control of Industrial Dryers*, 2007; Vol. 2, pp 597–610.
- [2] Dufour, P. Control Engineering in Drying Technology: Review and Trends. *Drying Technol.* **2006**, *24*, 889–904. DOI: [10.1080/07373930600734075](https://doi.org/10.1080/07373930600734075).
- [3] Abdel-Jabbar, N. M.; Jumah, R. Y.; Al-Haj Ali, M. State Estimation and State Feedback Control for Continuous Fluidized Bed Dryers. *J. Food Eng.* **2005**, *70*, 197–203. DOI: [10.1016/j.jfoodeng.2004.09.026](https://doi.org/10.1016/j.jfoodeng.2004.09.026).
- [4] Platt, D.; Palazoglu, A.; Rumsey, T. Feedforward-Feedback Control of a Cross-Flow Grain Dryer. *Hilg* **1992**, *60*, 1–27. DOI: [10.3733/hilg.v60n01p027](https://doi.org/10.3733/hilg.v60n01p027).
- [5] Courtois, F.; Nouafo, J.; Trysham, G. Control Strategies for Corn Mixed-Flow Dryers. *Drying Technol.* **1995**, *13*, 1153–1165. DOI: [10.1080/07373939508917014](https://doi.org/10.1080/07373939508917014).
- [6] McFarlane, N.; Bruce, D. A Cost Function for Continuous-Flow Grain Drying and Its Use in Control. *J. Agric. Eng. Res.* **1996**, *65*, 63–75. DOI: [10.1006/jaer.1996.0080](https://doi.org/10.1006/jaer.1996.0080).
- [7] Liu, Q.; Bakker-Arkema, F. W. A Model-Predictive Controller for Grain Drying. *J. Food Eng.* **2001**, *49*, 321–326. DOI: [10.1016/S0260-8774\(00\)00229-6](https://doi.org/10.1016/S0260-8774(00)00229-6).
- [8] Li, H.; Chen, S. A Neural-Network-Based Model Predictive Control Scheme for Grain Dryers. *Drying Technol.* **2020**, *38*, 1079–1091. DOI: [10.1080/07373937.2019.1611598](https://doi.org/10.1080/07373937.2019.1611598).
- [9] Jin, Y.; Wong, K. W.; Yang, D.; Zhang, Z.; Wu, W.; Yin, J. A Neural Network Model Used in Continuous Grain Dryer Control System. *Drying Technol.* **2022**, *40*, 1901–1922. DOI: [10.1080/07373937.2021.1891930](https://doi.org/10.1080/07373937.2021.1891930).
- [10] Mansor, H.; Noor, S.; Kamil, R.; Taip, F.; Farouq, O. Intelligent control of Grain Drying Process Using Fuzzy Logic Controller. *J. Food. Agric. Environ.* **2010**, *8*, 145–149.
- [11] Athajariyakul, S.; Leephakpreeda, T. Fluidized Bed Paddy Drying in Optimal Conditions via Adaptive Fuzzy Logic Control. *J. Food Eng.* **2006**, *75*, 104–114. DOI: [10.1016/j.jfoodeng.2005.03.055](https://doi.org/10.1016/j.jfoodeng.2005.03.055).
- [12] Hnin, K. K.; Zhang, M.; Mujumdar, A. S.; Zhu, Y. Emerging Food Drying Technologies with Energy-Saving Characteristics: A Review. *Drying Technol.* **2019**, *37*, 1465–1480. DOI: [10.1080/07373937.2018.1510417](https://doi.org/10.1080/07373937.2018.1510417).
- [13] Su, Y.; Zhang, M.; Mujumdar, A. S. Recent Developments in Smart Drying Technology. *Drying Technol.* **2015**, *33*, 260–276. DOI: [10.1080/07373937.2014.985382](https://doi.org/10.1080/07373937.2014.985382).
- [14] Martynenko, A.; Bück, A. *Intelligent Control in Drying*. CRC Press: Boca Raton, **2018**; Vol. 3.
- [15] Heath, J. A.; Kookos, I. K.; Perkins, J. D. Process Control Structure Selection Based on Economics. *AIChE J.* **2000**, *46*, 1998–2016. DOI: [10.1002/aic.690461012](https://doi.org/10.1002/aic.690461012).
- [16] Skogestad, S. Plantwide Control: The Search for the Self-Optimizing Control Structure. *J. Process Control* **2000**, *10*, 487–507. DOI: [10.1016/S0959-1524\(00\)00023-8](https://doi.org/10.1016/S0959-1524(00)00023-8).
- [17] Bottari, A.; Marchetti, P. A.; Marchetti, A. G. Self-Optimizing Steady-State Back-Off Approach for Control Structure Selection. *Ind. Eng. Chem. Res.* **2019**, *58*, 13699–13717. DOI: [10.1021/acs.iecr.8b06296](https://doi.org/10.1021/acs.iecr.8b06296).
- [18] Jäschke, J.; Cao, Y.; Kariwala, V. Self-Optimizing Control – A Survey. *Annual Reviews in Control* **2017**, *43*, 199–223. DOI: [10.1016/j.arcontrol.2017.03.001](https://doi.org/10.1016/j.arcontrol.2017.03.001).
- [19] Vasconcelos, L. G. S.; Maciel Filho, R. Development of a Supervisory Control Strategy for Optimal Operation of Grain Dryers. *Drying Technol.* **1998**, *16*, 2017–2031. DOI: [10.1080/07373939808917509](https://doi.org/10.1080/07373939808917509).
- [20] Bottari, A.; Zumoffen, D. A. R.; Marchetti, A. G. Economic Control Structure Selection for Two-Layered Real-Time Optimization Systems. *Ind. Eng. Chem. Res.* **2020**, *59*, 21413–21428. DOI: [10.1021/acs.iecr.0c02591](https://doi.org/10.1021/acs.iecr.0c02591).
- [21] Parry, J. L. Mathematical Modelling and Computer Simulation of Heat and Mass Transfer in Agricultural Grain Drying: A Review. *J. Agric. Eng. Res.* **1985**, *32*, 1–29. DOI: [10.1016/0021-8634\(85\)90116-7](https://doi.org/10.1016/0021-8634(85)90116-7).

- [22] Parde, S. R.; Jayas, D. S.; NDG White. Grain Drying: A Review. *Sci. Aliments* **2003**, 23, 589–622. DOI: 10.3166/sda.23.589-622.
- [23] Platt, D.; Rumsey, T.; P, A. Dynamics and Control of Cross-Flow Grain Dryers: I. Model Development and Testing. *Drying Technol.* **1991**, 9, 27–60. DOI: 10.1080/07373939108916640.
- [24] Platt, D.; Rumsey, T. R.; Palazoglu, A. P. Dynamic Modelling of a Cross-Flow Rice Dryer. *Hilg* **1990**, 58, 1–46. DOI: 10.3733/hilg.v58n04p046.
- [25] Siebenmorgen, T. J.; Jindal, V. K. Airflow Resistance of Rough Rice as Affected by Moisture Content, Fines Concentration and Bulk Density. *Trans. ASABE* **1987**, 30, 1138–1143.

Appendix A: Relative gain matrix equations

Let the full input-output gain matrix of the open loop system evaluated at the nominal optimum $\mathbf{u}^*(\mathbf{d}_n)$ be defined as $\mathbf{G} \in \mathbb{R}^{n_y \times n_u}$. Let $\mathbf{G}_s(\mathbf{z}) \in \mathbb{R}^{n_l \times n_l}$ be the square sub-matrix, with n_l loops, determined by the selected control structure. Then, the RGA bounding constraints approach aims to solve the followings equations for the controlled sub process:

$$\Lambda(\mathbf{z}) = \mathbf{G}_s(\mathbf{z}) \otimes [\mathbf{G}_s^{-1}(\mathbf{z})]^T \quad (\text{A1a})$$

$$\Lambda_p(\mathbf{z}, \mathbf{Z}^p) = \Lambda(\mathbf{z}) \otimes \mathbf{Z}^p(\mathbf{z}) \quad (\text{A1b})$$

$$\delta^L \leq \sum_{j=1}^{n_l} \lambda_{p,i,j}(\mathbf{z}, \mathbf{Z}^p(\mathbf{z})) \leq \delta^U, \quad i = 1, \dots, n_l \quad (\text{A1c})$$

$$\sum_{i=1}^{n_l} z_{i,j}^p = \sum_{j=1}^{n_l} z_{i,j}^p = 1 \quad (\text{A1d})$$

where $\Lambda(\mathbf{z})$ is the RGA matrix corresponding to the selected control structure \mathbf{z} ; $\mathbf{Z}^p \in \mathbb{B}^{n_l \times n_l}$ is the input-output pairing decision matrix (binary variables); the matrix $\Lambda_p \in \mathbb{R}^{n_l \times n_l}$ store the elements of the matrix Λ selected by \mathbf{Z}^p ;

$\lambda_{p,i,j}$ are the elements of the matrix Λ_p , $z_{i,j}^p$ are the elements of the matrix \mathbf{Z}^p , and δ^L and δ^U are the lower and upper bounds for the elements of the RGA matrix.

The values of δ^L and δ^U are design parameters that enforce a desired degree of interaction for the input-output loops. In this work the selected values are $\delta^L = 0.5$ and $\delta^U = 1.5$.

Appendix B: Nominal variables values

Table B1 show principal variable values for the optimal operation point in the defined nominal disturbance scenario.

The scaled version of process variables can then be calculated by:

$$M^* = \frac{M}{M_{in,n}}, \quad (\text{B1})$$

$$\theta^* = \frac{\theta - \theta_{in,n}}{T_{in,n} - \theta_{in,n}}, \quad (\text{B2})$$

$$W^* = \frac{W}{W_{in,n}}, \quad (\text{B3})$$

$$T^* = \frac{T - \theta_{in,n}}{T_{in,n} - \theta_{in,n}}, \quad (\text{B4})$$

$$G_a^* = \frac{G_a}{G_{a,n}}, \quad (\text{B5})$$

$$G_p^* = \frac{G_p}{G_{p,n}}, \quad (\text{B6})$$

$$h^* = \frac{h}{h_n}, \quad (\text{B7})$$

$$R^* = \frac{R}{R_n}. \quad (\text{B8})$$

Table B1. Nominal values (steady-state).

Process Variable	Type	Case Study	Dimension	Value
Inlet Air Temperature	u	$T_{in,n}$	[°C]	45
Dry Air Mass Velocity	u	$G_{a,n}$	[kg/s.m ²]	0.250
Dry Grain Mass Velocity	u	$G_{p,n}$	[kg/s.m ²]	2.135
Inlet Absolute Humidity of Air	d	$W_{in,n}$	[kg/kg _{dryair}]	0.009
Inlet Grain Temperature	d	$\theta_{in,n}$	[°C]	35
Inlet Moisture Content of Grain	d	$M_{in,n}$	[kg/kg _{drygrain}]	0.23
Convective heat transfer coeff.	var	h_n	[J/m ³ .s.°C]	14333
Drying rate	var	R_n	[kg _{water} /kg _{drygrain} .s]	$2.062 * 10^{-5}$
Operation Cost	Functional	J_n	[\$]/[ton _{drygrain}]	5.071